BENCHMARKING THE PENH MONTE CARLO CODE AGAINST PHITS: ASSESSMENT OF PROTON DEPTH-DOSE

Y. Kubyshin*, E. Marin†, J. Sempau‡, Universitat Politècnica de Catalunya, Barcelona, Spain

Abstract

This study provides a benchmark of the PENELOPE/PENH/PenEasy (2021 version) Monte Carlo code for proton transport using reference results from the established PHITS code. The comparison focuses on absorbed-dose distributions generated by a finite-spot proton pencil beam. Integrated depth-dose curves were simulated for energetic beams of 100 MeV and 226 MeV incident on a semi-infinite water phantom. The degree of agreement between PENH and PHITS is quantitatively assessed regarding the depth-dose behavior. The results evaluate PENH's accuracy and establish its suitability for general proton transport applications.

INTRODUCTION

Unlike conventional photon-based radiation therapy, proton radiotherapy offers a more pronounced dose profile characterized by the Bragg peak and a sharp distal dose falloff. These physical properties allow for highly conformal dose delivery to the tumor while minimizing damage to adjacent healthy tissue. However, because of this steep dose gradient, the precision of proton beam delivery is paramount in a clinical setting.

Monte Carlo (MC) simulations have been conducted by using the general-purpose radiation transport codes PENELOPE/PENH/PenEasy [1–4] (from now on PENH) and PHITS [5], which complements the benchmarking between PENH and PHITS conducted in [6].

This study follows a similar structure as Ref. [7], to benchmark various radiation transport codes, being PHITS among them.

PENH

The PENELOPE/PENH/PENEASY code represents a significant evolution in the Monte Carlo (MC) simulation code of radiation transport. The 2024 version of PENELOPE (PENetration and Energy Loss of Positrons and Electrons) has been extended to include proton interactions via the PENH library (2021 version). PENH introduces the necessary physics to model proton-matter interactions, including elastic scattering, electronic stopping, and nuclear reactions. This upgrade maintains the robust "mixed" simulation algorithm of its predecessor, combining hard events with multiple-scattering approximations to ensure both computational efficiency and high spatial accuracy. By integrating proton transport into the existing geometry and material handling systems of PENELOPE, PENH provides a versatile tool for applications in medical physics, such as proton therapy and space radiation protection. This unified approach allows for the simultaneous tracking of primary protons and their secondary electromagnetic cascades within complex geometries. Finally PENEASY (2024 version) provides the interface to launch the simulations.

* iouri.koubychine@upc.edu
† eduard.marin.lacoma@upc.edu
‡ josep.sempau@upc.edu

PHITS

The PHITS code version 3.35, was employed for the inter-code comparison. Nucleon-induced nuclear reactions were modeled by the INCL4.6 model [8]. For neutron energies below 20 MeV, the transport is based on the cross section data library, JENDL-5.0 [9]. Photon and electron transports were calculated by the PHITS built-in EGS5 [10] algorithm.

OBJECTIVES

The main goal is to validate the suitability of PENH to transport protons against the well established by the scientific community radiation transport code, PHITS. The study focuses on the absorbed-dose distributions in a water phantom for two scenarios, regarding the energy of the incident proton beam. The results obtained by PENH and PHITS for each scenario are presented and discussed.

SIMULATION FRAMEWORK

The simulated scenarios, the beam definition and the parameters of the Monte-Carlo simulation for both codes are presented below.

Scenarios

The Integrated Depth Dose Curves (IDDCs) of a pencil proton beam of two energies are considered in this study:

1. 100 MeV (Scenario-1) and,
2. 226 MeV (Scenario-2).

In both scenarios, a mono-energetic and mono-directional proton pencil beam enters a semi-infinite lateral extent water phantom. The depths of the water phantom for scenarios 1 and 2 are 10 cm and 40 cm, respectively, to capture the Bragg peak location.

The absorbed doses were scored by disks of 5 cm radius and 1 mm depth, distributed along the beam direction. The disk radius of 5 cm is chosen to capture all energy deposition. Figure 1 shows the dose obtained at the Bragg peak (blue data) as a function of the radius. Fitting a Gaussian curve to that profile leads to a 1-σ equal to (0.67 cm) which is almost a factor of 10 larger than the considered disks.

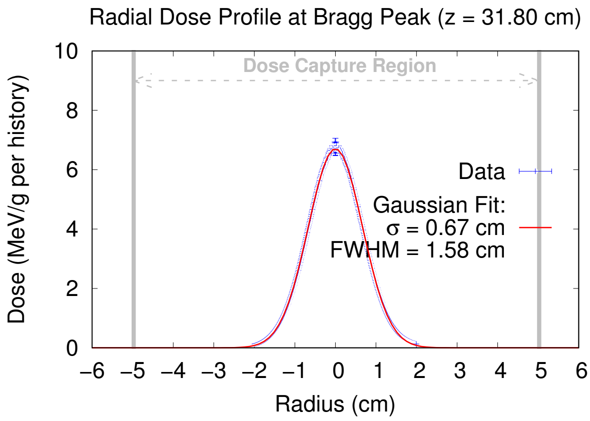

Figure 1: Energy deposition in the transverse plane observed at the Bragg Peak location for Scenario-2 (226 MeV). The vertical lines in gray color represent the disks of 5 cm radius used for evaluating the dose in the transverse plane.

Monte Carlo Simulations

The Monte Carlo simulation framework for both codes was configured to ensure a balance between physical accuracy and computational efficiency. Table 1 shows the considered cutoff energies for e^-/e^+, photons, protons and neutrons in both codes.

Table 1: Cutoff Energies Considered in the Monte-Carlo Simulations

Code	e^-/e^+ [keV]	**Photons [keV]**	**Protons [MeV]**	**Neutrons [eV]**
PENH	100	1	1	10^3
PHITS	100	1	1	10^{-5}

In PHITS, the simulation parameter *nspread* is set to 2 to account for energy dispersion in the Coulomb scattering or deceleration processes of charged particles, using the cutoff values shown in Table 1. In addition, the *ih2o* parameter, which controls the ionization potential of water [11], is set to 78.0 eV to match that one in PENH.

In both codes the defined tallies refer to the dose energy deposition along the direction of the incident proton beam. Hence the dose is integrated over the plane perpendicular to the beam trajectory in steps of 1 mm.

Finally the processor utilized in the simulations consists of a 11th Gen Intel(R) Core(TM) i7-11850H @ 2.50GHz, 2496 Mhz, 8 Core(s), 16 Logical Processors. Simulations carried out in PHITS exploits 4 cores, while simulations in PENH were not configured to run in parallel, despite the capabilities of the code.

SIMULATION RESULTS

The comparison between PENH and PHITS shows remarkably good agreement in the obtained dose profiles, Bragg peak location and sharp distal dose falloff. Tables 2 and 3 summarize the comparison between the codes in terms of Bragg peak and computation performance, respectively.The location of the peak is obtained at the bin where the maximum dose deposition is recorded.

Table 2: Comparison between PENH and PHITS simulation results for both energy scenarios. The Peak column refers to the position of the Bragg peak from the entrance of the water phantom. The Histories column refers to the number of simulated histories.

Code	**Energy [MeV]**	**Peak [cm]**	**Histories** [10^6]
PENH	100	7.60(5)	12.2
PHITS	100	7.60(5)	67.7
PENH	226	31.80(5)	3.0
PHITS	226	31.80(5)	41.4

Table 3: Comparison between PENH and PHITS simulation performance in terms of number of simulated histories, CPU time and speed simulation for both scenarios. Note that CPU time is the product of the simulation time times the number of cores.

Code	**Energy [MeV]**	**Histories** [10^6]	**CPU [min]**	**Speed** [10^3 **hist./s]**
PENH	100	12.2	124	1.47
PHITS	100	67.7	788	1.43
PENH	226	3.0	125	0.41
PHITS	226	41.4	1664	0.42

Scenario-1

For Scenario-1, both codes locate the Bragg peak at the same bin which is 7.6(5) cm from the entrance of the phantom. The uncertainty in the peak location comes from half of the width of the considered disk, being 1 mm, see Fig. 2. In terms of dose deposition at the Bragg peak, PHITS reports a value less than 1 % higher than PENH. Regarding computational efficiency, PENH shows approximately 2.8 % higher performance with respect to PHITS.

Scenario-2

In Scenario-2, the Bragg peak was observed at a greater depth, near 32 cm, see Fig 3. Quantitatively, the Bragg peak locations and dose levels reported in Table 2 show a remarkably good agreement between the codes.

However, the obtained dose profiles in the direction of propagation of the proton beam, show differences within the range that goes from 10 cm to 25 cm. The maximum difference over that range is always ≤5.7 %. Plausible explanations include:

- Energy straggling methods; sampling of the energy loss per step,
- Nuclear models and data libraries; PHITS uses INCL while PENH implements *ENDF-6*.

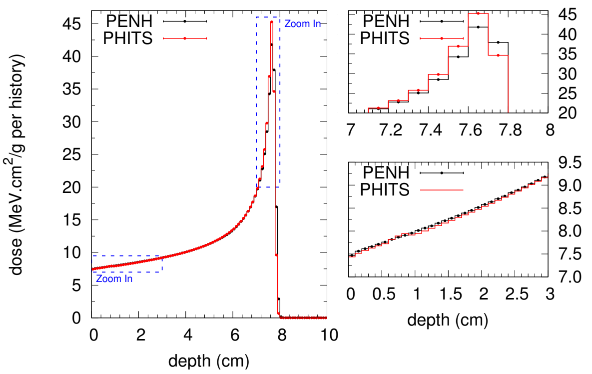

Figure 2: Deposition energy comparison of a mono-energetic beam of 100 MeV, between PENH (black) and PHITS (red). Right-side plots are zoom-in figures marked in blue dashed rectangles in left figure, to provide a more detailed view at the entrance of the phantom (bottom-right) and near the peak (top-right).

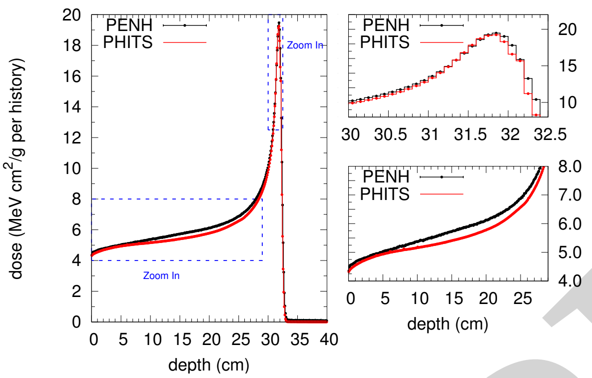

Figure 3: Deposition energy comparison of mono-energetic beam of 226 MeV, between PENH (black) and PHITS (red). Right-hand side plots are the zoom-in figures marked in blue dashed rectangles in the left figure.

Further studies would be required to explain the observed differences.

Regarding computational efficiency, again similar performances are observed between the codes, yet PHITS is 2.4% faster than PENH. When comparing the two scenarios, there is a penalization of 9.2 s for each MeV of energy increase at history level.

CONCLUSIONS

This benchmarking study successfully validated the PENH Monte Carlo code against the established PHITS code for proton transport applications in water phantoms. The results demonstrate an excellent agreement in the integrated depth-dose (IDDC) distributions for both 100 MeV and 226 MeV scenarios. Specifically, both codes accurately captured the entrance dose, the longitudinal straggling, and the precise location of the Bragg peak, which was found at 7.6 cm for the 100 MeV beam and at 31.8 cm for the 226 MeV in both codes. A small discrepancy is observed in the high energy case that shows in the intermediate region from depths between 10 cm and 25 cm but it is kept ≤5.7 %. In terms of simulation speed both codes shows almost same performance, differences are kept ≤3 %.

In conclusion, all primary objectives of this study have been successfully reached. The rigorous inter-comparison confirms that PENH provides reliable and precise proton transport modeling, establishing its suitability as an efficient and accurate tool for general applications in medical physics and radiation protection.

ACKNOWLEDGEMENTS

Financial support from grant PID2022-140503OB-I00 funded by the Spanish MICIU/AEI/10.13039/501100011033 and by ERDF/EU is gratefully acknowledged. YK is grateful to Tatsuhiko Ogawa for his insightful and detailed comments on the PHITS code.

REFERENCES

[1] F. Salvat, “A generic algorithm for Monte Carlo simulation of proton transport”, *Nucl. Instrum. Methods Phys. Res. B*, vol. B136, pp. 144-159, 2013. doi:10.1016/j.nimb.2013.08.035

[2] F. Salvat and J.M. Quesada, “Nuclear effects in proton transport and dose calculations”, *Nucl. Instrum. Methods Phys. Res. B*, vol. B475, pp. 49-62, 2020. doi:10.1016/j.nimb.2020.03.017

[3] F. Salvat, “PENELOPE-2018: A code system for Monte Carlo simulation of electron and photon transport”, OECD Nuclear Energy Agency, Rep. NEA/MBDAV/R(2019)1, Sept. 2019. https://www.oecd-nea.org/upload/docs/application/pdf/2020-10/penelope-2018__a_code_system_for_monte_carlo_simulation_of_electron_and_photon_transport.pdf

[4] J. Sempau, A. Badal, and L. Brualla, “A PENELOPE-based system for the automated Monte Carlo simulation of clinacs and voxelized geometries–application to far-from-axis fields”, *Med. Phys.*, vol. 38, pp. 5887-95, 2011. doi:10.1118/1.3643029

[5] T. Sato *et al.*, “Recent improvements of the Particle and Heavy Ion Transport code System – PHITS version 3.33”, *J. Nucl. Sci. Technol.* 61, 68-73 2023. doi:10.1080/00223131.2023.2275736

[6] Y. Kubyshin, E. Marin, and J. Sempau, “Benchmarking the PENELOPE/PENH and PHITS codes for calculation of beam quality correction factors in therapeutic proton beams”, presented at IPAC’26, Deauville, France, May 2026, paper WEP5129, this conference.

[7] Z.-Y. Yang *et al.*, “Inter-comparison of dose distributions calculated by FLUKA, GEANT4, MCNP, and PHITS for proton therapy”, *EPJ Web of Conf.*, vol. 153 p. 04011, 2017. doi:10.1051/epjconf/201715304011

[8] A. Boudard *et al.*, “New potentialities of the Liège intranuclear cascade model for reactions induced by nucleons and light charged particles”, *Phys. Rev. C*, vol. 87, p. 014606, 2013. doi:10.1103/PhysRevC.87.014606

[9] O. Iwamoto *et al.*, "Japanese Evaluated Nuclear Data Library Version 5: JENDL-5," *J. Nucl. Sci. Technol.*, vol. 54, no. 7, pp. 655–692, 2023. doi:10.1080/00223131.2022.2141903

[10] H. Hirayama *et al.*, "EGS5 (Electron Gamma Shower ver. 5)", SLAC National Accelerator Laboratory, Menlo Park, CA, USA, Rep. SLAC-R-730 & KEK 2005-8, Mar. 2006. https://rcwww.kek.jp/research/egs/egs5_manual/slac730-060330.pdf

[11] H. Weick *et al.*, "Improved accuracy of the code ATIMA for energy loss of heavy ions in matter", GSI, Darmstadt, Germany, Rep. ATIMA GSI Scientific Report 2017-5, 2017. https://web-docs.gsi.de/~weick/atima/ATIMA_GSI_scientific_report_2017-5.pdf